Synthesis and Characterization of Lithium, Sodium, and Potassium Porphyrin Complexes. X-ray Crystal Structures of $Li_2(C_6H_{12}O_2)_2TMPP$, $Na_2(THF)_4OEP$, and $K_2(pyridine)_4OEP$

John Arnold,* Denisha Y. Dawson, and Caroline G. Hoffman

Contribution from the Department of Chemistry, University of California, Berkeley, California 94720

Received October 26, 1992

Abstract: Reaction of free-base porphyrins (H_2Por = octaethylporphyrin (OEP), *meso*-tetraphenylporphyrin (TPP), *meso*-tetra-*p*-tolylporphyrin (TTP), *meso*-tetrakis(4-*tert*-butylphenyl)porphyrin (TBPP), *meso*-tetrakis(3,4,5-trimethoxyphenyl)porphyrin (TMPP)) with 2 equiv of $MN(SiMe_3)_2$ (M = Li, Na, K) in THF or dimethoxyethane (DME) yields dimetal salts of empirical formula $M_2(THF)_4Por$ and $M_2(DME)_2Por$, respectively. The lithium derivatives crystallize from donor solvents in the form of 1:1 salts $[Li(solv)_n][Li(Por)]$ (solv = THF, n = 4; solv = DME, diacetone alcohol, n = 2). The crystallography determined structure of the TMPP derivative crystallized from acetone consists of a $[Li(TMPP)]^-$ anion and a $[Li(diacetone\ alcohol)_2]^+$ counterion. ^7Li NMR spectroscopy and conductivity measurements suggest these ionic structures are retained in polar solvents; however, in relatively nonpolar solvents symmetrical ion-paired structures are observed. For the larger sodium ion, X-ray crystallography shows two $Na(THF)_2$ moieties symmetrically bound to all four nitrogens, one on each face of the porphyrin ring. The structure of the pyridine complex $K_2(pyr)_4(OEP)$ has also been determined; it is similar to the sodium salt but shows the solvent molecules positioned perpendicular to the porphyrin ring, presumably to maximize π-interactions between neighboring molecules in the crystal. X-ray data are as follows: $Li_2(C_6H_{12}O_2)_2$ (TMPP): $P\bar{1}$ with a = 12.420(2) Å, b = 12.965(2) Å, c = 13.998(2) Å, α = 66.29(2)°, β = 60.21(2)°, γ = 77.00(2)°, V = 1790 Å^3, d_{calc} = 1.23 g cm^{-3}, and Z = 1. $Na_2(THF)_4(OEP)$: $P\bar{1}$ with a = 9.801(3) Å, b = 11.598(3) Å, c = 12.106(2) Å, α = 96.81(2)°, β = 106.67(2)°, γ = 107.52(2)°, V = 1225 Å^3, d_{calc} = 1.18 g cm^{-3}, and Z = 1. $K_2(pyr)_4(OEP)$: $P\bar{1}$ with a = 10.102(4) Å, b = 13.974(5) Å, c = 19.029(4) Å, α = 89.88(2)°, β = 76.78(2)°, γ = 72.90(2)°, V = 2493 Å^3, d_{calc} = 1.24 g cm^{-3}, and Z = 2.

Introduction

Spectroscopic evidence for the formation of alkali metal porphyrin complexes $M_2(Por)$ was obtained as long ago as 1948 following treatment of pyridine solutions of tetraphenylporphyrin with alkali metal hydroxides.[1] Their synthetic potential was demonstrated a few years later when complete transmetalation of dilithium tetraphenylporphyrin (generated in situ) and metal acetates of zinc and mercury was monitored spectroscopically.[2] More recently, Buchler and co-workers described the in situ preparation of $Li_2(OEP)$ (generated from $H_2(OEP)$ and *n*-butyllithium in trichlorobenzene) to form metal sandwich compounds.[3,4] Prior to our work, however, there were no reports of isolable alkali metal porphyrins.[5-9] We became interested in compounds of this type for their potential use as reagents in the synthesis of porphyrin derivatives of the early transition metals and have described, in preliminary form, the preparation of the THF solvate of dilithium octaethylporphyrin, $[(THF)_4Li][Li(OEP)]$, and its metathesis reactions with metal halides to produce (OEP)ScCl and $(OEP)ZrCl_2$.[10-12] Here we give a full account of the preparation and characterization of this dilithium salt along with some related tetraaryl derivatives, including the X-ray structure of the TMPP complex. In addition, we report an extension of this chemistry to sodium and potassium derivatives and present the first detailed structural characterization of porphyrin complexes of these metals.

Results and Discussion

The general reaction scheme used to synthesize alkali metal complexes of OEP, TPP, TBPP, TTP, and TMPP is shown below.

$$H_2(Por) + 2MN(SiMe_3)_2 \xrightarrow[\text{reflux}]{\text{solv}} M_2(Por)(solv)_n + 2HN(SiMe_3)_2$$

(M = Li, Na, K; solv = THF, DME)

The metal silylamides are ideal reagents in this scheme as they are readily available in pure form, they are extremely soluble in the solvents shown above, and the amine byproduct does not interfere with subsequent purification of the desired product. By using this simple procedure, large-scale (5–10 g), high-yield syntheses of pure dialkali metal porphyrins are easily accomplished.

For the OEP compounds, a noticeable color change from brown to dark red was observed shortly after dissolution of the porphyrin, and the reaction was complete by UV/vis spectroscopy within 30

(1) Rothemund, P.; Menotti, A. M. *J. Am. Chem. Soc.* **1948**, *70*, 1808.
(2) Dorough, G. D.; Miller, J. R.; Huennekens, F. M. *J. Am. Chem. Soc.* **1951**, *73*, 4315.
(3) Buchler, J. W.; Hütterman, J.; Löffler, J. *Bull. Soc. Chem. Jpn.* **1988**, *61*, 71.
(4) Buchler, J. W.; De Cian, A.; Fischer, J.; Hammerschmitt, P.; Weiss, R. *Chem. Ber.* **1991**, *124*, 1051.
(5) Allison, J. B.; Becker, R. S. *J. Phys. Chem.* **1963**, *67*, 2675.
(6) Hambright, P. In *Porphyrins and Metalloporphyrins*; Smith, K. M., Ed.; Elsevier: New York, 1975; p 233.
(7) Buchler, J. W. In *The Porphyrins*; Dolphin, D., Ed.; Academic: New York, 1978; Vol. 1, p 390.
(8) Related alkali metal complexes of metalloporphyrins, such as $[Na(THF)_3]_2[Fe(TPP)]$ (Mashiko, T.; Reed, C. A.; Haller, K. J.; Scheidt, W. R. *Inorg. Chem.* **1984**, *23*, 3192) and $[Na(THF)_3]_2[Co(TPP)]$ (Ciurli, S.; Gambarotta, S.; Floriani, C.; Chiesi-Villa, A.; Guastini, C. *Angew. Chem., Int. Ed. Engl.* **1986**, *25*, 553) have been reported. In addition, a lithium porphyrinogen was described very recently: Jubb, J.; Floriani, C.; Chiesi-Villa, A.; Rizzoli, C. *J. Am. Chem. Soc.* **1992**, *114*, 6571.
(9) Mashiko, T.; Dolphin, D. In *Comprehensive Coordination Chemistry*; Wilkinson, G., Gillard, R. D., McCleverty, J. A., Eds.; Pergamon: Oxford, 1987; Chapter 21.
(10) Arnold, J. *J. Chem. Soc., Chem. Commun.* **1990**, 976.
(11) Arnold, J.; Hoffman, C. G. *J. Am. Chem. Soc.* **1990**, *112*, 8620.
(12) Brand. H.; Arnold, J. *J. Am. Chem. Soc.* **1992**, *114*, 2266.

0002-7863/93/1515-2707$04.00/0

Table I. UV–Visible Data for Alkali Metal Porphyrins

compd[a]	λ/nm (log ε)	solvent
H_2(OEP)	398 (5.2), 496 (4.1), 528 (4.0), 568 (3.8), 622 (3.8)	THF
Li_2(THF)$_4$(OEP)	332 (4.2), 416 (5.0), 552 (4.0), 588 (3.8)	THF
Na_2(THF)$_4$(OEP)	329 (4.0), 408 (5.0), 552 (3.8), 588 (3.3)	THF
K_2(THF)$_4$(OEP)	331, (4.1), 422 (4.6), 560 (3.9), 596 (3.2)	THF
H_2(TPP)[b]	417 (5.6), 515 (4.2), 552 (3.9), 594 (3.7), 650 (3.6)	CH_2Cl_2
Li_2(DME)$_3$(TPP)	434 (5.5), 574 (4.4), 614 (4.3)	DME
Li_2(TPP)[c]	456, 502 w, 534 w, 576, 619	pyridine
H_2(TMPP)	420 (5.5), 514 (4.2), 550 (3.9), 590 (3.8), 652 (3.7)	DME
Li_2(DME)$_2$(TMPP)	434 (5.6), 574 (4.3), 616 (4.1)	DME
Na_2(DME)$_n$(TMPP)	434 (5.6), 576 (4.1), 618 (4.1)	DME
K_2(DME)$_n$(TMPP)	434 (5.7), 574 (4.2), 616 (4.1)	DME
Li_2(DME)$_n$(TTP)	434 (5.5), 574 (4.4), 616 (4.3)	DME
Li_2(DME)$_n$(TBPP)	434 (5.6), 576 (4.3), 618 (4.2)	DME

[a] Data from this work unless stated otherwise. [b] Data from ref 7. [c] Data from ref 1.

min. In the lithium case, for example, the Soret band is red-shifted from 398 nm in H_2(OEP) to 416 nm in the product and the four Q-bands (496, 528, 568, 622 nm) are replaced by two new absorptions of similar intensity at 552 and 588 nm (see Table I). The latter change reflects the higher symmetry of the molecule upon metalation. Similar spectroscopic changes were observed for the aryl porphyrin derivatives, where the solutions rapidly took on an emerald green cast as viewed by reflected light and a bluish-violet hue by transmitted light. We note that Li_2(TPP) had been generated in situ many years ago and that our spectra for the isolated compound are in good agreement with the earlier data.[1] The sodium and potassium analogs display very similar features to the lithium compounds, as shown in Table I. The complexes are quite stable as solids but, as expected, they are moisture sensitive, with hydrolysis back to the free-base porphyrin being rapid and quantitative as determined by UV/vis spectroscopy and preparative-scale reactions.

As is generally the case in porphyrin chemistry, the OEP derivatives are much more soluble than their tetraaryl counterparts. Among the latter, the TMPP derivatives are the most soluble, with the TPP species being poorly soluble in all solvents examined. The alkali metal also influences solubility properties, such that the lithium salts of all porphyrins were more soluble than either the sodium or potassium analogs, with the latter displaying rather similar solubilities. Accordingly, we found it necessary to concentrate and cool the reaction solutions in order to isolate the OEP salts, with the resulting dark red needles of pure Li, Na, or K compounds typically being obtained in >90% yields. In contrast, the tetraarylporphyrin salts rapidly precipitated from the solution as insoluble bluish-purple powders, but again yields were high. For the TMPP species, crystalline products were obtained by layering a solution of the amide over a solution of the porphyrin in the same solvent. The TPP and TTP sodium and potassium compounds may be prepared by the above procedure, but their exceedingly low solubilities precluded full characterization.

Following isolation by filtration and drying under a rough vacuum, most of the crystalline compounds rapidly lost coordinated solvent, and elemental analyses were of no practical use in gauging either product purity or composition. Using ^{1}H NMR spectroscopy, however, the amount of solvent remaining was easily determined. For example, the vacuum dried Li_2(OEP) product shows a THF/OEP ratio of approximately 2:1, whereas for freshly isolated, nondried samples this was nearer the value of 4:1 determined by X-ray crystallography (see below). This solvent lability does not affect subsequent reactivity and the original product can be regenerated quantitatively by dissolution and crystallization from THF. For subsequent synthetic use, however, it is convenient to determine the composition in order to calculate an effective molecular weight.

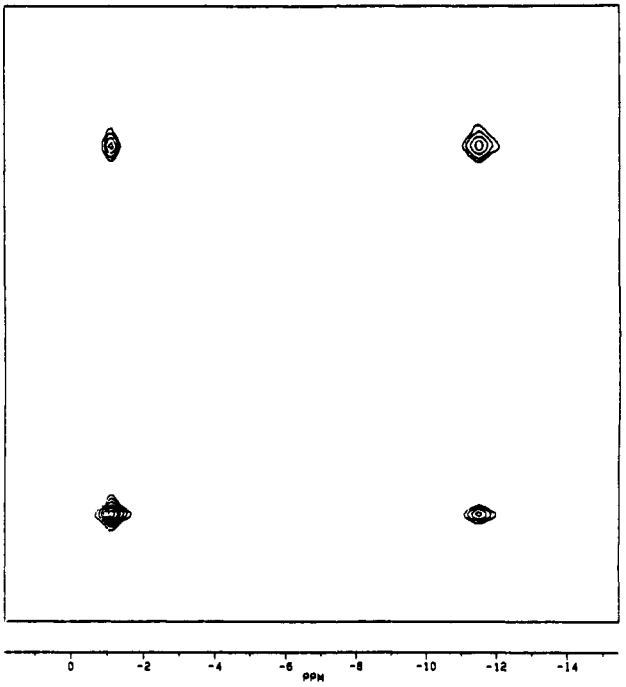

Figure 1. ^{7}Li NOESY spectrum of Li_2(TMPP) in DMSO-d_6 at 41 °C.

For the lithium compounds, ^{7}Li NMR spectroscopy provides firm evidence for solution structures that are solvent dependent. For example, in DMSO, Li_2(TMPP) shows two equal-intensity signals at 25 °C (−1.12 ppm ($\nu_{1/2}$ = 4 Hz) and −11.55 ppm ($\nu_{1/2}$ = 52 Hz)) that broaden before finally coalescing to a single peak (−6 ppm) on warming to 100 °C. The results of a ^{7}Li NOESY experiment (Figure 1), which show the cross-peaks expected for a two-site exchange process, also suggest that rapid lithium exchange is occurring under these conditions. Qualitatively similar results were observed in acetone but the coalescence temperature (−13 °C) was much lower in this solvent. Low-temperature ^{7}Li NMR spectra of Li_2(TPP) and Li_2(TBPP) in acetone at −60 °C showed analogous behavior, with one relatively sharp singlet at −11 ppm, a broader peak at 0.4 ppm, and a coalescence temperature of −15 °C. Assuming a simple two-site exchange process,[13] this behavior corresponds to an activation energy of 10 ± 1 kcal mol^{-1} at −15 °C.

Considering both the positions and linewidths of these peaks, we assign the sharper, lower field signal to a lithium ion surrounded by a spherically-symmetrical array of solvent molecules and the broader, more shielded peak to a lithium ion coordinated to the four porphyrin nitrogens in a square-planar environment.[14] Note that large upfield shifts such as those observed here are uncommon as the ^{7}Li chemical shift range normally spans only ±2 ppm. High-field shifts of this magnitude are generally associated with strong shielding by π-electron density[15]—in this case from the porphyrin ligand.[16] In solvents of much lower polarity, such as THF, benzene, and tetramethylethylenediamine (TMEDA), the OEP complex shows only a single relatively sharp temperature

(13) Lukehart, C. M. *Fundamental Transition Metal Organometallic Chemistry*; Brooks/Cole: Monterey CA, 1985; p 200.

(14) As ^{7}Li is quadrupolar ($I = 3/2$), sharper lines indicate a more spherically symmetrical field around the nucleus. In general, the shifts of tetrahedrally coordinated species are relatively insensitive to the nature of the solvent. See: Dechter, J. J. *Prog. Inorg. Chem.* **1982**, *29*, 285 and references therein.

(15) Similar solvent effects have been described in ^{7}Li NMR of several aromatic ion pairs. See, for example: (a) Cox, R. H.; Terry, H. W. *J. Magn. Reson.* **1974**, *14*, 317. (b) Elschenbroich, C. A.; Salzer, A. *Organometallics*; VCH: New York, 1989; p 26. Cyclopentadienyllithium, for example, exists as contact ion pairs in THF (δ −8.37 ppm) and as predominately solvent separated ion pairs in hexamethylphosphoramide (δ −0.88 ppm).

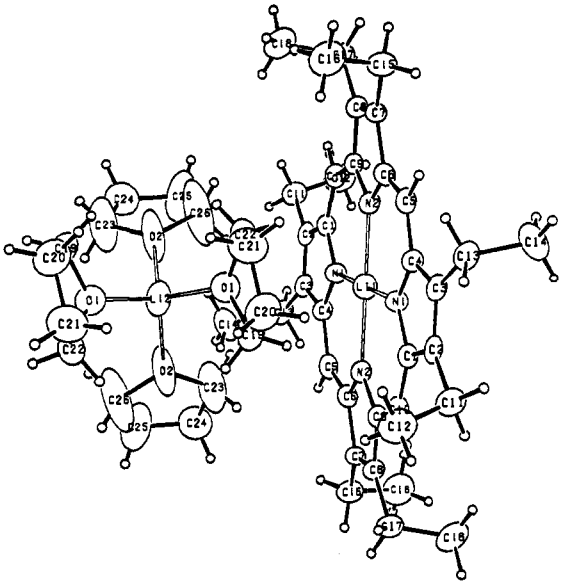

Figure 2. ORTEP drawing of $Li_2(THF)_4(OEP)$.

independent $^7Li\{^1H\}$ signal at −12.8 ppm in THF and −16.5 ppm in benzene and TMEDA. In contrast to the ionic structure proposed above, we interpret these data as evidence for a covalent structure in which the lithiums are bound symmetrically, as in **A** and **B** below.

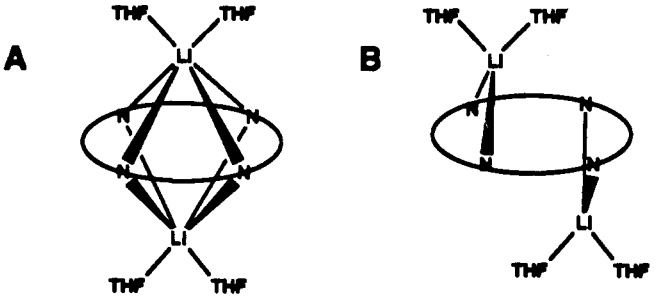

X-ray data for the sodium and potassium OEP compounds show that structure **A** is plausible; nevertheless, due to the much smaller ionic radius of lithium and its lower average coordination number, the arrangement shown in **B** is also quite possible.

Conductivity measurements on $Li_2(OEP)$ provide additional valuable information as to the solvent dependence of the solution structure. Thus, in acetonitrile and acetone, conductivities are in the range expected for a 1:1 electrolyte; in THF, however, the complex is virtually non-conducting.[17] These data are in accord with the ^7Li NMR results and are interpreted as further evidence for a solvent-separated ion pair complex in polar solvents such as DMSO or acetone, and a contact ion pair structure in less polar solvents such as THF and TMEDA.

X-ray Structural Studies

Li_2(TMPP). Large needles of the TMPP complex were obtained from acetone. The structure is similar to that for the OEP derivative, $[(THF)_4Li][Li(OEP)]$[10] (shown in Figure 2 for comparison), consisting of $Li(solv)^+$ cations and $Li(OEP)^-$ anions. A view of the anion (Figure 3) shows the square-planar lithium ion at the center of the N_4 porphyrin ring. There are no out-of-plane close contacts, and Li–N bond lengths (Li–N 2.031(2), 2.044(2) Å, Table II) are identical with those determined for the OEP case (Li–N 2.032(3), 2.042(3) Å). The $[Li(TMPP)]^-$ anion is crystallographically centrosymmetric and very planar (maximum deviation 0.02 Å). The aryl groups are also very planar and are inclined approximately perpendicular to the porphyrin ring. To our knowledge, the only other example of a square-planar lithium was found in the phthalocyanine radical, Li(pc), where the Li–N bond length is 1.942(5) Å.[18]

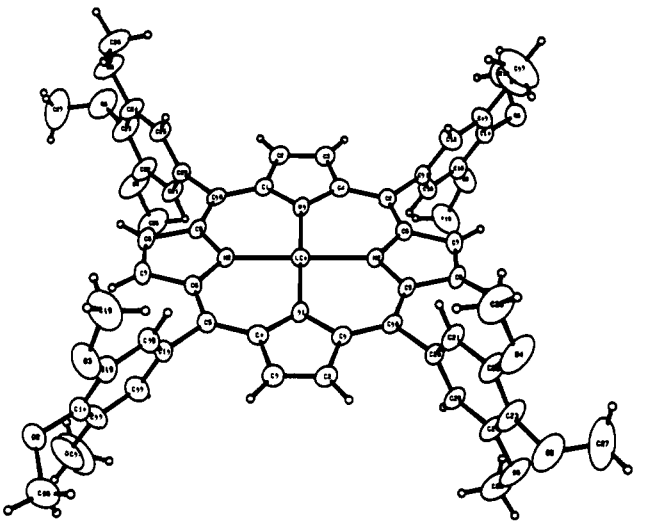

Figure 3. ORTEP drawing of the anion $[Li(TMPP)^-]$ in $Li_2(C_6H_{12}O_2)_2(TMPP)$.

Table II. Data for $Li_2(C_6H_{12}O_2)_2(TMPP)$

Selected Bond Distances (Å)			
Li1–N1	2.031(2)	Li1–N2	2.044(2)
Li2–O5	2.240(9)	Li2–O7	2.138(9)
Li2–O7	1.943(9)	Li2–O8	2.316(9)
Li2–O8	2.059(9)	Li2–O8′	1.988(9)
Li2–O8′	2.403(10)	Li2–Li2	1.56(2)
N1–C1	1.368(3)	N1–C4	1.372(3)
N2–C6	1.362(3)	N2–C9	1.373(3)
Selected Intramolecular Angles (deg)			
N1–Li1–N1	180.0	N1–Li1–N2	89.54(7)
N1–Li1–N2	90.46(7)	N2–Li1–N2	180.0
C1–N1–C4	105.97(16)	C6–N2–C9	106.16(17)
C4–C5–C6	124.92(19)	C1–C10–C9	126.15(19)
O5–Li2–O7	107.9(4)	O5–Li2–O7	116.7(4)
O5–Li2–O8	119.9(4)	O5–Li2–O8	100.5(4)
O5–Li2–O8′	96.7(4)	O7–Li2–O7	135.4(4)
O7–Li2–O8	76.3(3)	O7–Li2–O8	84.2(3)
O7–Li2–O8′	87.6(3)	O7–Li2–O8′	88.1(4)
O7–Li2–O8	82.2(3)	O7–Li2–O8	87.0(4)
O8–Li2–O8	138.7(4)	O8–Li2–O8′	162.6(5)

The second lithium ion is coordinated in a roughly square-pyramidal fashion by two molecules of diacetone alcohol (the aldol addition product of acetone) and by the methoxy oxygen of one of the trimethoxyphenyl groups (Figure 4). (The origin of the alcohol has not been determined precisely, but we note that traces were detected in the acetone used to recrystallize the sample). Due to the inversion center, each of these cations is surrounded by four porphyrins in a plane, and the Li2 atom is disordered between coordination to one or the other of the available porphyrins. In addition, the hydroxyls are apparently hydrogen bonded to one of the methoxy oxygens (O2) of two porphyrin molecules (the latter being different from the porphyrin to which the Li is bonded). The Li–O and OH···O bonds link three of the four porphyrins around each inversion center at any given location and on average all four are linked. This arrangement forms infinite linked planes of the two ions that are stacked normal to the planes

(16) For discussions of diamagnetic anisotropy of ring currents in porphyrins see, for example: (a) Janson, T. R.; Katz, J. J. In *The Porphyrins*; Dolphin, D., Ed.; Academic: New York, 1978; Vol. IV, p 38. (b) Scheer, H.; Katz, J. J. In *Porphyrins and Metalloporphyrins*; Smith, K. M., Ed.; Elsevier: New York, 1975; Chapter 10. (c) Guilard, R.; Lecomte, C.; Kadish, K. M. *Struct. Bond.* **1987**, *64*, 205.

(17) Geary, W. J. *Coord. Chem. Rev.* **1971**, *7*, 81.

(18) Sugimoto, H.; Mori, M.; Masuda, H.; Taga, T. *J. Chem. Soc., Chem. Commun.* **1986**, 962.

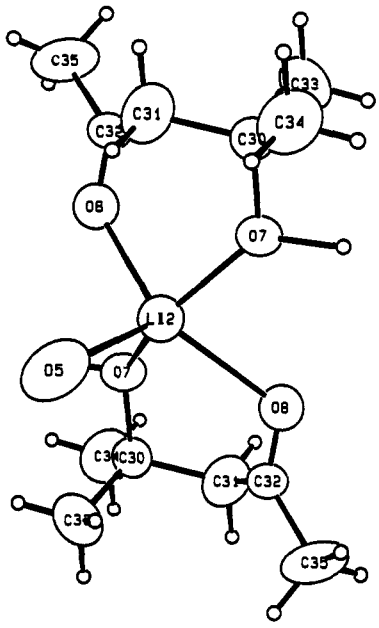

Figure 4. ORTEP drawing of the cation in $Li_2(C_6H_{12}O_2)_2(TMPP)$.

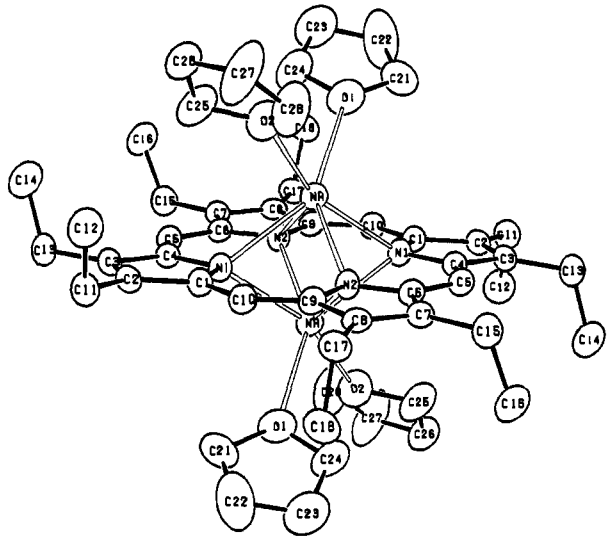

Figure 5. ORTEP drawing of $Na_2(THF)_4(OEP)$.

in such a way as to locate the cation above the central plane of a porphyrin of the adjoining level. This packing leaves holes in the unit cell and these are filled by a disordered acetone molecule (see supplementary material for a view of the disorder model).

Na_2(OEP). In contrast to the two ion-paired lithium compounds described above, the THF solvate of the sodium derivative exists as discrete molecules in the solid state (Figure 5). There is only half of each molecule in the asymmetric unit, and the molecule is strictly centrosymmetric (space group $P\bar{1}$). Each six-coordinate sodium ion is bound to all four nitrogen atoms of a slightly ruffled porphyrin (Na–N 2.452, 2.508(2) Å, Table III), with the oxygens from two THF's completing the distorted trigonal prismatic coordination (Na–O 2.417, 2.400(2) Å). (For comparison, the corresponding distances in $[Na(THF)_3]_2$-[Fe(TPP)][19] in which the sodiums are bound to *two* porphyrin nitrogens and *three* THF oxygens are the following: Na–N 2.784(4), 2.825(4) Å and Na–O 2.311(4)–2.339(4) Å). The distance from the sodium to the N_4 plane is 1.38 Å. The THF's are severely distorted by a combination of thermal motion and disorder; they are bent away from each other apparently to help fill the void between molecules in the unit cell.

(19) Mashiko, T.; Reed, C. A.; Haller, K. J.; Scheidt, W. R. *Inorg. Chem.* **1984**, *23*, 3192.

Table III. Data for $Na_2(THF)_4(OEP)$

Selected Bond Distances (Å)			
Na–N1	2.452(2)	Na–N1	2.508(2)
Na–N2	2.469(2)	Na–N2	2.479(2)
N1–C1	1.367(2)	N1–C4	1.366(2)
N2–C6	1.369(2)	N2–C9	1.368(2)
Selected Intramolecular Angles (deg)			
N1–Na–N1′	112.21(5)	N1–Na–N2	72.16(6)
N1–Na–N2′	72.46(6)	N1′–Na–N2	71.69(6)
N1′–Na–N2′	71.05(6)	N2–Na–N2′	112.03(5)
O1–Na–O2	79.02(6)	O1–Na–N1	92.89(6)
O1–Na–N2	143.66(7)	O1–Na–N1′	143.58(7)
C4–C5–C6	128.0(2)	C1–C10–C9	128.4(2)
C1–N1–C4	106.4(2)	C6–N2–C9	106.1(2)

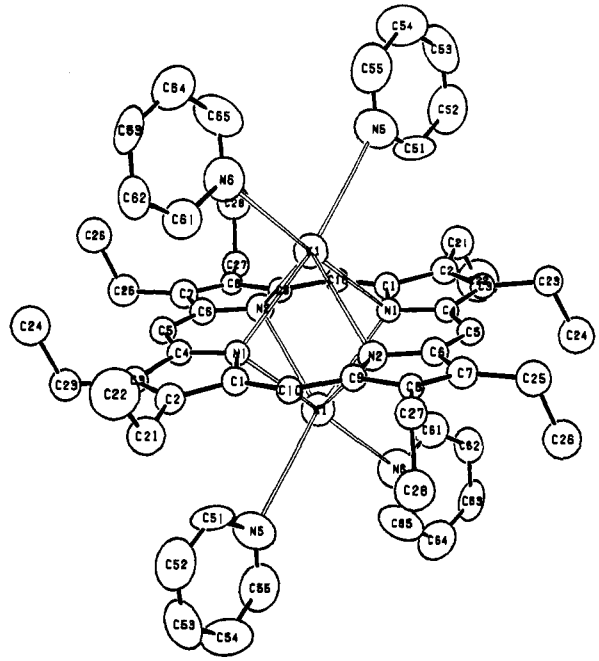

Figure 6. ORTEP drawing of $K_2(pyr)_4(OEP)$.

Table IV. Data for $K_2(pyr)_4(OEP)$ (Molecule 1)

Selected Bond Distances (Å)			
K1–N1	2.740(7)	K1–N1	2.794(6)
K1–N2	2.757(7)	K1–N2	2.790(8)
K1–N5	3.017(9)	K1–N6	2.961(8)
N1–C1	1.410(10)	N1–C4	1.355(10)
N2–C6	1.332(11)	N2–C9	1.390(10)
Selected Intramolecular Angles (deg)			
N1–K1–N1	96.4(2)	N1–K1–N2	64.7(2)
N1–K1–N2	63.3(2)	N1–K1–N5	92.1(2)
N2–K1–N5	119.5(2)	N2–K1–N5	121.4(2)
N5–K1–N6	86.0(2)	N2–K1–N2	96.6(2)
C1–N1–C4	106.7(6)	C6–N2–C9	107.4(7)
C4–C5–C6	125.3(8)	C1–C10–C9	130.6(7)

K_2(OEP). The structure is qualitatively similar to the sodium derivative, with the larger six-coordinate alkali metal located 1.84 Å above the OEP plane. There are two independent, centrosymmetric molecules in the triclinic ($P\bar{1}$) unit cell that differ mainly in the disposition of the ethyl groups and extent of ruffling in the OEP ring, with molecule 1 (Figure 6; Table IV) being slightly ruffled and molecule 2 effectively planar. The planes of the two porphyrins are not parallel, with an angle of 7.9° between them. The orientation of the solvent molecules is the major difference between the sodium and potassium structures. In the latter, the pyridines are nearly perpendicular to the OEP plane—an arrangement no doubt enforced by packing considerations illustrated in Figure 7. The molecules pack very well in this configuration, in a manner difficult to imagine if the pyridines

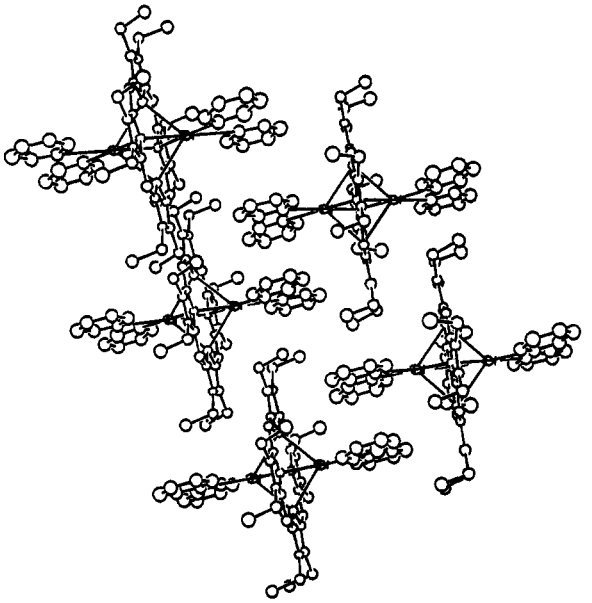

Figure 7. Packing diagram of $K_2(pyr)_4(OEP)$.

were oriented as in the sodium/THF case. This packing also seems to dictate the "eclipsed" conformation of the pyridines with respect to the pyrrole nitrogens. The two sets of K–N bond lengths show the expected trends, with distances from the OEP nitrogens to the potassium being ca. 0.25 Å shorter than those to the pyridines. Inspection of angles around potassium suggests its coordination is better described as cubic with two vacant sites, rather than trigonal prismatic or antiprismatic.

Experimental Section

All manipulations were carried out under nitrogen or argon unless stated otherwise. Tetrahydrofuran (THF), diethyl ether, toluene, hexane, and dimethoxyethane (DME) were predried over 4-Å molecular sieves and distilled from sodium/benzophenone under N_2. Dichloromethane was distilled from calcium hydride under N_2. Acetone was dried over 4-Å molecular sieves and then distilled under N_2. All NMR solvents were treated similarly but were distilled under vacuum. TMEDA was distilled from sodium under argon. TPP, TMPP, TBPP, and TTP were prepared by the usual reaction of pyrrole with the corresponding benzaldehyde in refluxing propionitrile.[20] Proton NMR spectra were referenced to tetramethylsilane at δ 0.00 ppm. Lithium-7 NMR data were referenced to external 0.3 M LiCl in MeOH at δ 0 ppm with a spectrometer frequency of 194.37 MHz. The ^{7}Li NOESY data were measured in DMSO-d_6 with t_1 incremented in 256 steps and the data zero-filled to 512 words before Fourier transformation; eight scans were recorded for each increment with t_{mix} = 5 ms and a relaxation time of 200 ms. Elemental analyses and mass spectra (EI, 70 eV) were performed at the departmental facility of the College of Chemistry, University of California, Berkeley.

$Li_2(THF)_4(OEP)$. A 1000-mL round-bottom Schlenk flask equipped with a magnetic stirring bar was charged with 5.00 g of $H_2(OEP)$ (9.35 mmol) and a 3.500 g of $LiN(SiMe_3)_2$ (20.96 mmol). THF (500 mL) was transferred by cannula into the reaction vessel and the mixture was heated to reflux for 3.5 h over which time the solution gradually became homogeneous and deep magenta in color. The solution was filtered while hot, concentrated under reduced pressure to ca. 100 mL, and diluted with an equal volume of hexane. The mixture was cooled to –40 °C over 8 h to give dark red, needle-like crystals (mp >320 °C) in 95% yield (6.14 g) that were isolated by filtration. The complex rapidly loses approximately 2 equiv of THF at room temperature as determined by integration of the ^{1}H NMR spectrum; the following empirical formula is based on this composition. Anal. Calcd for $C_{44}H_{60}N_4O_2Li_2$: C, 76.5; H, 8.75, N, 8.11. Found: C, 77.8; H, 9.33; N, 7.89. ^{1}H NMR (300 MHz, acetone-d_6 20 °C): δ 1.78 (m, 8H, THF), 1.90 (t, J = 8 Hz, 24H, $-CH_2CH_3$), 3.62 (m, 8H, THF), 4.01 (q, J = 8 Hz, 16H, $-CH_2CH_3$), 9.77 (s, 4H, –C*H*–). ^{7}Li{^{1}H} NMR (acetone-d_6, 25 °C): δ –3.9 (v br s). Conductivity data: (acetone, 2.7 mM, 20 °C) ΛM = 100 Ω^{-1} cm^2 mol^{-1}; (MeCN, 5.7 mM, 20 °C) ΛM = 93 Ω^{-1} cm^2 mol^{-1}; (THF, 3.7 mM, 20 °C) ΛM = 0.11 Ω^{-1} cm^2 mol^{-1}.

$Li_2(DME)_3(TPP)$. DME (40 mL) was added by cannula to a mixture of $H_2(TPP)$ (1.00 g, 1.60 mmol) and $LiN(SiMe_3)_2$ (0.59 g, 3.53 mmol). A reflux condenser was attached under a counterflow of argon and the reaction mixture was heated at reflux with stirring for 8 h. The solution was cooled to room temperature and then filtered to obtain 1.27 g (92%) of a bright purple powder that was dried in vacuo for several hours, mp >450 °C. ^{1}H NMR (400 MHz, acetone-d_6, 20 °C): δ 3.37 (s, 12H, DME), 3.54 (s, 18H, DME), 7.75 (m, 12H, $-C_6H_5$), 8.27 (m, 8H, $-C_6H_5$), 8.63 (s, 8H, –C*H*–). ^{7}Li{^{1}H} NMR (acetone-d_6, –60 °C): δ –10.95 (s, 1 Li), 0.35 (s, 1 Li). Anal. Calcd for $C_{56}H_{58}N_4O_6Li_2$: C, 74.99; H, 6.52; N, 6.25. Found: C, 75.26; H, 6.29; N, 6.17.

$Li_2(DME)_n(TBPP)$. DME (35 mL) was added to a mixture of $H_2(TBPP)$ (1.00 g, 1.52 mmol) and $LiN(SiMe_3)_2$ (0.550 g, 3.29 mmol). A reflux condenser was attached under a counterflow of argon and the reaction mixture was heated at reflux with stirring for 12 h. The reaction mixture was allowed to cool to room temperature and then filtered. The solid was dried in vacuo to remove residual solvent, leaving 0.87 g of a bright purple microcrystalline material. The filtrate was concentrated to ca. 20 mL and allowed to cool to –40 °C, affording a second crop of 0.06 g for a total yield of 0.93 g (80%), mp >450 °C. ^{1}H NMR (400 MHz, acetone-d_6, 20 °C): δ 1.70 (s, 36H, $-C(CH_3)$), 3.38 (s, DME), 3.54 (s, DME), 7.84 (d, J = 88 Hz, 8H, C_6H_4), 8.24 (d, J = 9 Hz, 8H, C_6H_4), 8.68 (s, 8H, C*H*). ^{7}Li{^{1}H} NMR (acetone-d_6, –70 °C): δ –11.0 (s, 1 Li), 0.2 (s, 1 Li).

$Li_2(DME)_n(TTP)$. DME (30 mL) was added to a mixture of $H_2(TTP)$ (0.50 g, 0.74 mmol) and $LiN(SiMe_3)_2$ (0.260 g, 1.55 mmol). A reflux condenser was attached under a counterflow of argon and the reaction mixture was heated with stirring at reflux for 8 h. The resulting homogeneous maroon solution was filtered while still warm into a Schlenk tube. Hexane (10 mL) was added to the filtrate and the mixture was cooled to –40 °C, affording large bright purple needles that crumbled upon exposure to vacuum (0.53 g, 80.5%), mp >450 °C. ^{1}H NMR (250 MHz, acetone-d_6, 20 °C): δ 2.76 (s, 12H, $-CH_3$), 3.38 (s, DME), 3.55 (s, DME), 7.60 (d, J = 8 Hz, 8H, C_6H_4), 8.18 (d, J = 8 Hz, 8H, C_6H_4), 8.65 (s, 8H, C*H*).

$Li_2(DME)_2(TMPP)$. A 500-mL round-bottom Schlenk flask equipped with a magnetic stirring bar was charged with 5.00 g of $H_2(TMPP)$ (5.13 mmol) and 1.716 g of $LiN(SiMe_3)_2$ (10.3 mmol). A 350-mL portion of DME was transferred by cannula into the reaction vessel. The solution was stirred at reflux for 2.5 h during which time it gradually became homogeneous. By reflected light, the solution was distinctly teal, whereas transmitted light appeared violet. After being allowed to cool to room temperature, the solution was filtered into a Schlenk tube and concentrated under reduced pressure to 150 mL. An equal volume of pentane was added and, after standing at –40 °C for 15 h, 5.05 g of product (mp >350 °C) was isolated (88%). Anal. Calcd for $C_{64}H_{72}N_4O_{16}Li_2$: C, 65.9; H, 6.22; N, 4.80. Found: C, 65.8; H, 5.91; N, 4.86. ^{1}H NMR (400 MHz, acetone-d_6, 20 °C): δ 3.27 (s, 12H, DME), 3.44 (s, 8H, DME), 3.96 (s, 24H, $C_6H_2(OMe)_3$), 4.03 (s, 12H, $C_6H_2(OMe)_3$), 7.49 (s, 8H, $C_6H_2(OMe)_3$), 8.64 (s, 8H, C*H*). ^{7}Li{^{1}H} NMR (acetone-d_6, 25 °C): δ –3.9 (v br s). ^{7}Li{^{1}H} NMR (DMSO-d_6, 25 °C): δ –11.55 (s, 1 Li), –1.12 (s, 1 Li). The sample used for elemental and X-ray analysis was recrystallized from acetone.

$Na_2(THF)_4(OEP)$. Using a procedure identical with that described for [$(THF)_4Li$][Li(OEP)] above, $H_2(OEP)$ (0.20 g, 0.37 mmol) in THF was treated with $NaN(SiMe_3)_2$ (0.14 g, 0.77 mmol). Workup as above yielded 0.20 g of purple needles that crumbled to a purple powder after several hours at room temperature. Proton NMR analysis of the dried material in acetone-d_6 showed an approximate stoichiometry of $Na_2(THF)_4(OEP)$. Crystals used in the structure determination were recrystallized from THF and quickly mounted on the diffractometer before noticeable solvent loss could occur.

$Na_2(DME)_n(TMPP)$. A 100-mL Schlenk tube was charged with 0.500 g (0.513 mmol) of $H_2(TMPP)$ and 35 mL of DME. In a separate flask, 0.188 g (1.03 mmol) of $NaN(SiMe_3)_2$ was dissolved in 15 mL of DME. The $NaN(SiMe_3)_2$ solution was transferred by cannula and layered onto the top of the porphyrin solution. The Schlenk tube containing both solutions was allowed to stand undisturbed for a week until the amide had diffused through the porphyrin layer. The compound formed has a distinctive emerald green cast in solution when viewed by reflected light. A 0.472-g sample of bluish-purple cube-like crystals of $Na_2(DME)_n(TMPP)$ was isolated, mp >350 °C. ^{1}H NMR (500 MHz, DMSO-d_6, 20 °C): δ 3.22 (s, DME), 3.40 (s, DME), 3.87 (s, 24 H,

(20) Adler, A. D.; Longo, F. R.; Finarelli, J. D.; Goldmacher, J.; Assour, J.; Korsakoff, L. *J. Org. Chem.* **1967**, *32*, 476.

Table V. Summary of Crystallographic Data

compd	$Li_2(C_6H_{12}O_2)_2(TMPP)$	$Na_2(THF)_4(OEP)$	$K_2(pyr)_4(OEP)$
formula	$O_{18}N_4C_{74}Li_2H_{78}$	$Na_2O_4N_4C_{52}H_{76}$	$K_2N_8C_{56}H_{64}$
mol wt	1325.3	867.2	927.4
cryst size, mm	0.40 × 0.50 × 0.60	0.22 × 0.24 × 0.52	0.17 × 0.26 × 0.47
space group	$P\bar{1}$	$P\bar{1}$	$P\bar{1}$
a, Å	12.420(2)	9.801(3)	10.102(4)
b, Å	12.965(2)	11.598(3)	13.974(5)
c, Å	13.998(2)	12.106(2)	19.029(4)
α, deg	66.29(2)	96.81(2)	89.88(2)
β, deg	60.21(2)	106.67(2)	76.78(2)
γ, deg	77.00(2)	107.52(2)	72.90(2)
vol, Å^3	1790	1225	2493
Z	1	1	2
d_{calcd}, g cm^{-3}	1.23	1.18	1.24
radiation, Å	Mo Kα 0.71073	Mo Kα 0.71073	Mo Kα 0.71073
scan mode	θ–2θ	θ–2θ	Ω
2θ range, deg	3–45	3–45	3–45
collection range	$+h,\pm k,\pm l$	$+h,\pm k,\pm l$	$+h,\pm k,\pm l$
abs coeff (μ), cm^{-1}	0.8	0.8	2.3
no. of unique reflns	4655	3198	6491
no. of reflns	$F^2 > 3\sigma(F^2)$: 3383	$F^2 > 3\sigma(F^2)$: 2291	$F^2 > 2\sigma(F^2)$: 3025
final R, R_w	0.0614, 0.0783	0.0461, 0.0548	0.0925, 0.0905
T, °C	–85	–87	–92

$C_6H_2(OMe)_3$), 3.97 (s, 12H, $C_6H_2(OMe)_3$), 7.40 (s, 8H, $C_6H_2(OMe)_3$), 8.66 (s, 8H, CH). ^{1}H NMR (300 MHz, acetone-d_6, 20 °C): δ 3.26 (s, DME), 3.44 (s, DME), 3.94 (s, 24H, $-C_6H_2(OMe)_3$), 4.03 (s, 12H, $C_6H_2(OMe)_3$), 7.46 (s, 8H, $C_6H_2(OMe)_3$), 8.72 (s, 8H, CH).

$K_2(Pyr)_4(OEP)$. Using a procedure similar to that described for the lithium and sodium salts of OEP above, $H_2(OEP)$ (0.15 g, 0.28 mmol) in THF was treated with $KN(SiMe_3)_2$ (0.12 g, 0.59 mmol). Workup as above yielded 0.14 g of deep purple plates. Due to its low solubility in THF, this material was much harder to manipulate than its lithium or sodium analogs. Fortunately, however, the salt is quite soluble in pyridine and recrystallization from a pyridine/hexane mixture afforded large needles of $K_2(pyr)_4(OEP)$ suitable for X-ray analysis.

$K_2(DME)_n(TMPP)$. A 100-mL Schlenk tube was charged with 0.500 g (0.513 mmol) of $H_2(TMPP)$ and 35 mL of DME. In a separate Schlenk flask, 0.188 g (1.03 mmol) of $KN(SiMe_3)_2$ was dissolved in 15 mL of DME. The $KN(SiMe_3)_2$ solution was transferred by cannula and layered onto the top of the porphyrin solution. The Schlenk tube containing both solutions was allowed to stand undisturbed for a week until the amide had diffused through the porphyrin layer. The compound formed has a distinctive emerald green cast in solution when viewed by reflected light. A 0.417-g sample of bluish-purple granular $K_2(DME)_n(TMPP)$ was isolated, mp >350 °C.

X-ray Crystallography

Table V lists a summary of crystallographic data for all three structurally characterized compounds. General operating procedures were as previously described.[21] Crystals were covered with a layer of Paratone-N hydrocarbon oil, removed from the drybox, inspected, and mounted on glass fibers as described by Hope.[22] Structure determinations were carried out by Dr. Hollander, Staff Crystallographer, CHEXRAY, University of California, Berkeley.

$[Li(C_6H_{12}O_2)_2][Li(TMPP)]$. Data were collected on a large deep-red needle crystallized from acetone at –85 °C. Automatic peak search and indexing yielded a triclinic reduced primitive cell; inspection of Niggli values revealed no conventional cell of higher symmetry. The 4655 unique raw data were converted to structure factor amplitudes and their esd's by correction for scan speed, background, and Lorentz and polarization effects. Inspection of the intensity standards showed a reduction of 8% of the original intensity for which the data were corrected. Inspection of the azimuthal scan data showed a variation $I_{min}/I_{max} = 0.82$ for the average curve; an empirical correction was applied to the data. The choice of the centric space group was confirmed by the successful solution and refinement of the structure. The structure was solved by direct methods (SHELXS)[23] in $P\bar{1}$ and refined by least-squares and Fourier techniques. The disordered solvent "puddle" was modeled by defining all atoms as carbon and refining their positions with a single isotropic thermal parameter for all. In a difference Fourier map calculated following refinement of all non-hydrogen atoms (except the solvent) with anisotropic thermal parameters, peaks were found corresponding to the positions of some hydrogens. Hydrogens were assigned idealized locations with values of B_{iso} approximately 1.2 times the B_{eqv} of the atoms to which they were attached; they were included in the structure factor calculations, but they were not refined. The hydrogen atom on the OH of the diacetone alcohol was included at the position it was found on the difference Fourier map. Six low-angle reflections with abnormally large weighted residuals were given zero weight in the final refinement. Inspection of the residuals ordered in ranges of $\sin\theta/\lambda$, $|F_0|$, and parity and value of the individual indexes showed no unusual features or trends. The largest peak in the final difference Fourier map had an electron density of 0.62 e Å^{-3}; the lowest was –0.27 e Å^{-3}. There was no evidence of secondary extinction in the high-intensity low-angle data.

$Na_2(THF)_4(OEP)$. The crystal used for low-temperature data collection (–87 °C) was grown from THF at –40 °C. Automatic peak search and indexing yielded a triclinic reduced primitive cell; inspection of Niggli values revealed no conventional cell of higher symmetry. The 3198 unique raw data were converted to structure factor amplitudes and their esd's by correction for scan speed, background, and Lorentz and polarization effects. No correction for crystal decomposition was necessary. Inspection of the azimuthal scan data showed a variation $I_{min}/I_{max} = 0.94$ for the average curve; an empirical correction was applied to the data. The choice of the centric space group ($P\bar{1}$) was confirmed by the successful solution and refinement of the structure. The structure was solved by SHELXS and refined by least-squares and Fourier techniques. In the difference Fourier map calculated following refinement of all non-hydrogen atoms with anisotropic thermal parameters, peaks were found corresponding to positions of most of the hydrogens; they were assigned idealized locations with values of B_{iso} approximately 1.2 times the B_{eqv} of the atoms to which they were attached and were included in the structure factor calculations, but they were not refined. In the final cycles of refinement a secondary extinction parameter was included (maximum correction was 13% on F). Inspection of the residuals

(21) Bonasia, P. J.; Arnold, J. *Inorg. Chem.* **1992**, *31*, 2508.
(22) Hope, H. In *Experimental Organometallic Chemistry*; Wayda, A. L., Darensbourg, M. Y., Eds.; ACS Symp. Ser. No. 357; American Chemical Society: Washington, DC, 1987; p 257.
(23) Sheldrick, G. M. *Crystallographic Computing 3*; Oxford University: Oxford, 1985; p 175.

ordered in ranges of sin θ/λ, $|F_o|$, and parity and value of the individual indexes showed no unusual features or trends. The largest peak in the final difference Fourier map had an electron density of 0.26 e Å^{-3}; the lowest was −0.08 e Å^{-3}.

K_2(pyr)$_4$(OEP). Purple blades were crystallized from pyridine at −20 °C. A fragment from a larger crystal was mounted on the diffractometer at −92 °C for data collection. Automatic peak search and indexing yielded a triclinic reduced primitive cell; inspection of Niggli values revealed no conventional cell of higher symmetry. The 6491 unique raw data were converted to structure factor amplitudes and their esd's by correction for scan speed, background, and Lorentz and polarization effects. No correction for crystal decomposition was necessary. Inspection of the azimuthal scan data showed a variation $I_{min}/I_{max} = 0.69$ for the average curve; an empirical correction was applied to the data. The choice of the centric space group ($P\bar{1}$) was confirmed by the successful solution and refinement of the structure. The structure was solved by Patterson methods and refined by least-squares and Fourier techniques. In a difference Fourier map calculated following refinement of some non-hydrogen atoms with anisotropic thermal parameters, peaks were found corresponding to positions of most of the hydrogens; they were assigned idealized locations with values of B_{iso} approximately 1.15 times the B_{eqv} of the atoms to which they were attached and were included in the structure factor calculations, but they were not refined. Before the final refinement cycles, 43 reflections were removed from the data set as they exhibited anomalously high background counts. The positional parameters of all non-hydrogen atoms were refined with anisotropic thermal parameters for the potassiums and atoms in the pyridines; atoms in the porphyrin were refined with isotropic thermal parameters because attempts to refine them otherwise led to physically unreasonable values. Inspection of the residuals ordered in ranges of sin θ/λ, $|F_o|$, and parity and value of the individual indexes showed no unusual features or trends. The largest peak in the final difference Fourier map had an electron density of 0.56 e Å^{-3}; the lowest was −0.17 e Å^{-3}. There was no evidence of secondary extinction in the high-intensity low-angle data.

Acknowledgment. We thank Dr. Mark Gallop for his invaluable help with the ^{7}Li NMR experiments, the Department of Education for a fellowship (to C.G.H.), and the National Physical Sciences Consortium for a fellowship (to D.Y.D.).

Note Added in Proof: The interaction of dodecaphenylporphyrin with lithium iodide was recently reported to yield the corresponding porphyrin–dilithium salt. See: Tsuchiya, S. *J. Chem. Soc., Chem. Commun.* **1992**, 1475.

Supplementary Material Available: Tables of temperature factor expressions, positional parameters, intramolecular distances and angles, least-squares planes, and anisotropic thermal parameters (37 pages); listings of observed and calculated structure factors (85 pages). Ordering information is given on any current masthead page.